Surface Science 604 (2010) 84–88

Contents lists available at ScienceDirect

Surface Science

journal homepage: www.elsevier.com/locate/susc

Signatures of epitaxial graphene grown on Si-terminated 6H-SiC (0 0 0 1)

Nikhil Sharma [a], Doogie Oh [b], Harry Abernathy [c], Meilin Liu [c], Phillip N. First [a,*], Thomas M. Orlando [a,b,*]

[a] School of Physics, Georgia Institute of Technology, Atlanta, GA 30425, United States
[b] School of Chemistry and Biochemistry, Georgia Institute of Technology, Atlanta, GA 30425, United States
[c] School of Materials Science and Engineering, Georgia Institute of Technology, Atlanta, GA 30425, United States

ARTICLE INFO

Article history:
Received 5 June 2009
Accepted for publication 15 October 2009
Available online 23 October 2009

Keywords:
Graphene
Silicon carbide
Raman spectroscopy
Scanning tunneling microscopy

ABSTRACT

Epitaxial graphene layers thermally grown on Si-terminated 6H-SiC (0 0 0 1) have been probed using Auger electron spectroscopy, Raman microspectroscopy, and scanning tunneling microscopy (STM). The average multilayer graphene thickness is determined by attenuation of the Si ($L_{23}VV$) and C (KVV) Auger electron signals. Systematic changes in the Raman spectra are observed as the film thickness increases from one to three layers. The most striking observation is a large increase in the intensity of the Raman 2D-band (overtone of the D-band and also known as the G′-band) for samples with a mean thickness of more than ~1.5 graphene layers. Correlating this information with STM images, we show that the first graphene layer imaged by STM produces very little 2D intensity, but the second imaged layer shows a single-Lorentzian 2D peak near 2750 cm^{-1}, similar to spectra acquired from single-layer micromechanically cleaved graphene (CG). The 4–10 cm^{-1} higher frequency shift of the G peak relative to CG can be associated with charge exchange with the underlying SiC substrate and the formation of finite size domains of graphene. The much greater (41–50 cm^{-1}) blue shift observed for the 2D-band may be correlated with these domains and compressive strain.

1. Introduction

Graphene, a two-dimensional hexagonal network of carbon atoms arranged in a trigonal planar geometry with sp^2 hybridization, has received significant attention from the physics, chemistry, materials science, and electrical engineering communities. Charge carriers in an ideal graphene sheet behave like massless Dirac fermions and possess potentially useful electronic properties. After interesting electric field effects were reported in cleaved graphene (CG) sheets [1], half-integer quantum Hall effects, and exotic transport properties have been probed experimentally [2,3] and described theoretically [4,5]. CG sheets are difficult to locate and pattern, thus their ultimate utility for electronic devices is limited. A parallel path for the creation of large-area graphene has been pursued for its potential value to nanoelectronics [6,7]. These methods produce single-layer or few-layer epitaxial graphene (EG) on SiC substrates [6–9]. This approach would allow integration into existing device fabrication paradigms.

The electronic behavior and surface structure/geometry of epitaxial single-layer or few-layer graphene on SiC (0 0 0 1) (the Si-terminated face) have been examined using surface sensitive techniques such as scanning tunneling microscopy (STM) [10], atomic force microscopy (AFM) [8], angle-resolved photoelectron spectroscopy (ARPES) [11–13], X-ray scattering [7,14,15], and Raman spectroscopy [16–20]. The characteristics and properties of the carbon-rich buried interface layer have also been examined using primarily X-ray scattering [15] and ARPES [9,21–23] measurements. The ARPES data indicate that a carbon-rich interface layer contains largely sp^2-bonded carbon, with the graphene π electrons bonded to substrate orbitals [9].

Raman spectroscopy can be used to distinguish and characterize CG since this material has a very characteristic G-band peaked at ~1590 cm^{-1} and a 2D-band (G′) at ~2720 cm^{-1}. The G peak is due to a one phonon process involving Γ-point optical phonons, and is characteristic of sp^2-bonded carbon, while the 2D peak results from a two-phonon resonant scattering process [24]. The presence of the 2D peak can indicate electronic structure which is dominated by Dirac–Weyl dispersion and is used as the typical signature for the presence of single-layer graphene [25]. As a consequence, recent Raman studies of epitaxial graphene grown on SiC [16–20] are beginning to provide crucial information concerning the intrinsic doping levels of the interface and compressive strain in the overlayer film. However, to date these studies have not correlated the Raman data with spatially resolved maps of the size and domain structures involved in the growth of these films. In this paper, we provide further information regarding the Raman optical signatures of epitaxial graphene grown on Si-terminated 6H-SiC

* Corresponding authors. Address: School of Physics, Georgia Institute of Technology, Atlanta, GA 30425, United States. Tel.: +1 404 894 4012 (T.M. Orlando).
E-mail addresses: First@physics.gatech.edu (P.N. First), Thomas.Orlando@chemistry.gatech.edu (T.M. Orlando).

0039-6028/$ - see front matter © 2009 Elsevier B.V. All rights reserved.
doi:10.1016/j.susc.2009.10.014

(0 0 0 1) as a function of film thickness and directly correlate this optical information with STM images. This allows us to collectively examine the importance of domain size and compressive strain as well as the role of charge exchange with the underlying substrate on the optical signatures of epitaxial single-layer and few-layer graphene.

2. Experiment

All EG samples were grown under ultrahigh vacuum (UHV) conditions. During UHV (base pressure $<1 \times 10^{-10}$ Torr) growth, it is possible to control the mean epitaxial graphene layer thickness by adjusting the growth temperature and time. Samples are prepared on *n*-doped 6H-SiC (0 0 0 1) substrates [26] that are etched at ~1500 °C in 1-atm of 5% H_2/95% Ar gas mixture to remove scratches from the surface. The substrate is then annealed in UHV by electron-bombardment heating (max pressure $\sim 10^{-8}$ Torr) at a temperature of 1200 °C producing a $(6\sqrt{3} \times 6\sqrt{3})$ R30° reconstruction. EG then grows by thermal desorption of Si at temperatures >1200 °C. Low-energy electron diffraction (LEED), Auger electron spectroscopy (AES) and room temperature scanning tunneling microscopy (STM) measurements are done *in situ* after growth. All STM data was acquired using chemically-etched tungsten probe tips at a constant tunneling current of 100 pA, unless otherwise indicated. Raman measurements are done *ex situ* in a Renishaw RM 1000 Raman microscope at a fixed laser wavelength of 514.5 nm (2.41 eV) and exit power below 3 mW. The laser is focused on the EG/SiC surface to ~1 μm diameter spot using a 50× objective. Under these conditions, spectral features scale linearly with the laser intensity. For background subtraction, Raman spectra are acquired from an ungraphitized control sample by focusing the laser into the SiC bulk below the surface. A reference sample of highly ordered pyrolytic graphite (HOPG) obtained from SPI supplies [27] was also studied.

3. Results and discussion

Fig. 1 shows the Auger spectra for three EG/SiC (0 0 0 1) samples studied in this work and presents a schematic of our present understanding of this system as inferred from low-temperature STM [10], photoemission spectroscopy [21], and X-ray scattering studies [15]. Changes are observed in the shapes of the Auger spectra, and in the relative intensities of the Si ($L_{23}VV$) and C (KVV) Auger features (see figure caption) as a function of annealing temperature. The effective thickness of the EG film is estimated using an attenuation model of the Si:C Auger intensities. Model results have been published previously [8] and described in detail [28]. Briefly, we model the dN/dE peak-to-peak intensity of Si Auger electrons emitted at 92 eV relative to the C Auger intensity at 272 eV. Assuming Gaussian Auger peaks in the energy distribution of emitted electrons $N(E)$, the peak-to-peak amplitude in $dN(E)/dE$ is proportional to the emitted flux of Auger electrons [29]. The model presumes exponential attenuation of the normal-incidence 3-keV excitation beam and the exiting Auger electrons (detected 42.2° from the surface normal) with inelastic mean free paths for electrons in graphite and SiC [30]). Elemental sensitivity and backscattering factors are taken from Ertl [29]. Three models were considered: (1) *n* layers of C at the graphene surface density (graphene-equivalent monolayers, ML_e) on bulk-terminated SiC, (2) *n* ML_e on SiC terminated by C adatoms at 1/3 the density of C in a SiC bilayer, and (3) *n* ML_e on SiC terminated by Si adatoms at 1/3 the density of Si in a SiC bilayer (models 2 and 3 explore the effect of a $\sqrt{3} \times \sqrt{3}$ or $6\sqrt{3} \times 6\sqrt{3}$ interface reconstruction). Differences among the models are small; at a Si:C intensity ratio of 0.45 (nominally 1 ML_e), the disparity is ±0.1 ML and decreases for smaller ratios (larger thickness).

The Auger thickness model is sensitive to layer densities only. It does not distinguish electronic properties, which are essential to the label "graphene". We will show that a consistent interpretation of available data indicates that the interface region (layer 0 or buffer layer) is carbon rich, but with electronic structure that is different from graphene. The buffer layer and overlying graphene layers can be distinguished in STM images by the intensity of interface states and by the amplitude of the 6×6 (referenced to the SiC surface unit cell) corrugation of the graphene; i.e. generically by the imaged roughness. However, because the detailed structure of the interface region is not yet known, in this paper we use ML_e to describe the film thickness determined by Auger attenuation. Based on current understanding, the carbon content of the interface region is close to that of a single graphene monolayer, therefore the mean number of graphene monolayers (ML) is less than ML_e by approximately 0.8 layer.

Fig. 2 shows Raman spectra acquired from the SiC bulk and from samples with graphene-equivalent thicknesses of 1.8 ML_e and 2.7

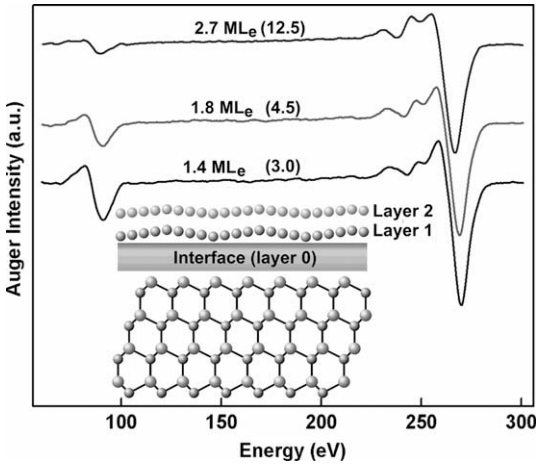

Fig. 1. Auger spectra of 1.4, 1.8 and 2.7 ML_e thick samples. The Auger electron spectra for epitaxial graphene samples show spectral changes in the Si ($L_{23}VV$) and C (KVV) peaks as a function of thickness. Changes can be seen in the relative intensities (in parentheses) of the C and the Si peaks which are used to calculate the sample thickness. The Si and C peaks are observed at 92 and 272 eV, respectively. The inset shows a schematic of the epitaxial graphene/SiC material system. The interface region influences the characteristics of epitaxial graphene layers.

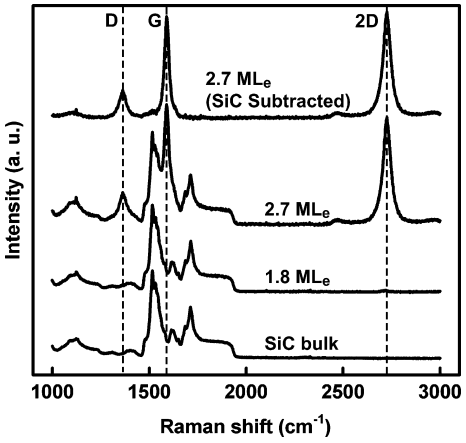

Fig. 2. Raman spectra showing the subtraction of the SiC background from the Raman raw data. Spectra for SiC and two different graphene coverages (1.8 ML_e and 2.7 ML_e) are shown, and one (2.7 ML_e) after subtraction. The SiC-band extends from ~1000 cm^{-1} to 2000 cm^{-1}. Changes after subtraction can be traced by following the dashed lines. D-, G- and 2D-bands are identified at 1420 cm^{-1}, 1590 cm^{-1} and 2720 cm^{-1}, respectively, for the 2.7 ML_e sample after the subtraction. Relatively small intensity of the 2D peak for the 1.8 ML_e sample is observed.

ML_e. Spectra are normalized to have equal intensity at the SiC edge near 1950 cm^{-1}. In the 2.7 ML_e sample, clear differences are observed from the other two spectra. There are additional pronounced peaks near 1420, 1590, and 2720 cm^{-1}. To isolate these features, the SiC background was subtracted from all spectra. The background-subtracted 2.7 ML_e spectrum is shown for comparison in Fig. 2. Three major peaks are identified as due to graphene [25,31]: the D mode near 1420 cm^{-1}, the G mode at ~1590 cm^{-1}, and the 2D (G′) mode near 2720 cm^{-1}. As mentioned previously, the G peak is due to a one phonon process involving Γ-point optical phonons, and is characteristic of sp^2-bonded carbon [25], while a single-Lorentzian 2D peak has been shown to be a signature of single-layer graphene [25]. The 2D peak for the 2.7 ML_e sample is well-fit by a single-Lorentzian with a full-width-at-half-maximum (FWHM) of 47 cm^{-1} (the FWHM of the 2D peak for mechanically exfoliated graphene is known to be approximately 30 cm^{-1}). The D peak or the breathing mode is due to a resonance process involving two inequivalent K and K′ points in the Brillouin zone of graphene [24]. The D peak is not allowed in ideal graphene due to the large wave-vector of the K-point phonon involved. Its presence is an indication of disorder, such as finite size domains [32], atomic scale defects and armchair-type edge defects [33]. The D- and 2D-bands are respectively, one-phonon + elastic scattering and two-phonon double resonance processes.

The 2.7 ML_e sample has approximately 68% layer 2 coverage. The Raman spectrum for this sample is therefore dominated by contribution from layer 2. There are fluctuations in the domain size and layer distribution; thus in this system, the intensity of the 2D peak cannot be used as a tool for thickness measurement [25]. The presence of the D peak is an indication of disorder in the system. Employing the empirical relationship between domain size and laser energy [32]

$$L_a\,(\mathrm{nm}) = \left(2.4\times10^{-10}\right)\lambda_{\mathrm{laser}}^4\left(\frac{I_D}{I_G}\right), \tag{1}$$

where I_D and I_G are integrated intensities; the lower bound of the mean domain size produced under our typical growth conditions is 32 nm.

The Raman spectrum for five different EG thicknesses (1.4, 1.8, 2.2, 2.7, and 3.3 ML_e) in addition to a spectrum on HOPG are shown in Fig. 3. Despite the large background subtraction, there is some evidence of the D and G peaks but no signal from the 2D peak for the 1.4 ML_e sample. It should be noted that STM-imaging (discussed below) shows that the 1.4 ML_e sample has only layer 0 and layer 1 coverage. For 1.8 and 2.2 ML_e samples, there is fractional coverage of layer 2 (13% and 27%, respectively) and some intensity is observed from the 2D mode. A dramatic jump in the 2D intensity is observed for the 2.7 ML_e sample (see Fig. 3). This coincides with a substantial increase in the fractional coverage of layer 2 (68%) on the surface, and the appearance of a small amount of layer 3 (7%). Consequently, we associate the dramatic increase in 2D Raman intensity with the graphene in layers 2 and higher. The observation of a single-Lorentzian 2D peak in samples dominated by layer 2 suggests similarities between this EG layer and single-layer CG. This conclusion, that the *second* graphene layer is similar to single-layer CG, is consistent with the substantial differences in STM-imaging of layer 1 and layer 2, as described below. Note that when the coverage is predominantly layer 2, the graphene overlayer is essentially continuous, even over steps in the substrate [8]. This could enhance the contribution of layer 2 versus layer 1 in the spectra.

We also observe that the Raman peaks are shifted to higher energy as compared to Raman peaks from CG. The G- and 2D-band shifts relative to both cleaved single-layer graphene and HOPG are shown in Fig. 4a. For undoped graphene, the average position of the G-band is expected at 1580 cm^{-1}. In our samples there is an upshift for the G peak of ~8 cm^{-1} which seems to be only

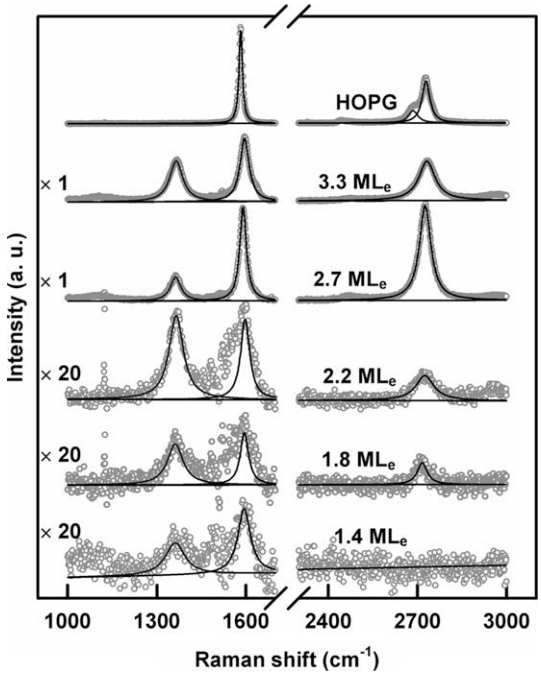

Fig. 3. Raman spectra for 1.4, 1.8, 2.2, 2.7, 3.3 ML_e and HOPG samples. The SiC background spectrum is subtracted from the raw data. Raman data for all EG samples has been normalized to the most intense SiC Raman feature. The 1.4 ML_e sample shows no evidence of the 2D peak. A sharp rise in intensity is observed for the 2D peak in the 2.7 ML_e sample. The 2D peak in the Raman spectra for HOPG is clearly different from the single-Lorentzian observed in EG.

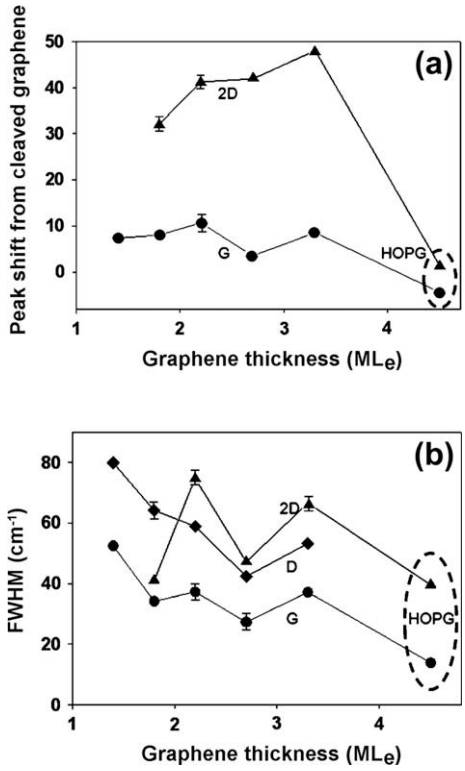

Fig. 4. (a) Peak shift for G and 2D peaks with respect to analogous peaks in the Raman spectra of single-layer exfoliated graphene on SiO_2. The peak positions for the single-layer exfoliated graphene samples were obtained from [25]. (b) Plot of the FWHM of the D, G and 2D peaks for 1.4, 1.8, 2.2, 2.7 and 3.3 ML_e samples.

weakly dependent on thickness, and is likely due to a combination of doping and disorder effects. In doped systems there is change in the Fermi surface and this moves the Kohn anomaly. Since the Fermi surface does not follow the Dirac cone displacement, this also leads to stiffening of the G mode phonons for both hole- and electron-doping [34]. Electrochemical gating was employed by Das et al. [35] to reach high doping levels (up to $5 \times 10^{13}\,\mathrm{cm}^{-2}$). In these measurements, phonon stiffening was observed for the G peak, whereas the 2D peak shows phonon softening ($20\,\mathrm{cm}^{-1}$) for higher gate voltage. A considerable shift to higher frequency ($50\,\mathrm{cm}^{-1}$) for the 2D-band is also shown in Fig. 4 and this shift seems to be maximum near 2.7 ML_e. The shift does not indicate phonon softening; rather it has been associated with compressive strain [19].

The Raman peak widths also change as a function of film thickness, as shown in Fig. 4b. Using the D or 2D peak energy width Γ as a measure of the mean excitation lifetime $\tau = \hbar/\Gamma$ produces estimates of the hot-carrier transport path length that are close to the measured domain sizes. The mean transport length can be estimated as $v_F\tau/2$ assuming ballistic transport up to the lifetime limiting event, or as $\sqrt{(D\tau)}$ for diffusive transport (elastic scattering time τ_e much less than τ), where $D = v_F^2\tau_e/2$ is the carrier diffusion constant. Taking $\tau_e = 10$ fs (see Ref. [12]) and a peak width of $50\,\mathrm{cm}^{-1}$ gives transport lengths of 50 nm (ballistic limit) and 25 nm (diffusive limit), which are comparable to measurements of the domain size from the D/G intensity ratio (see Eq. (1)), from surface X-ray scattering [14], and as shown below, from STM. Consequently, for films under two graphene layers, the excitation lifetime appears to be limited by domain size and defects. For thicker films, the peak width is thought to include a contribution also from multilayer peak splitting plus strain [17].

Note that we see only a weak G-band and no 2D features for the first graphene layer grown on Si-terminated SiC (0 0 0 1). This is contrast to the strong Raman bands seen for single-layer CG on a SiO_2 substrate. In cleaved graphene, only the phonons having $q > K$ contribute significantly towards the double resonance process. Kurti et al. [36] suggest that due to trigonal warping, $q < K$ involves an even portion of phase space and $q \sim K$ does not contribute at all to this process because of zero electron–phonon coupling [37,38]. It is possible that for layer 1, the bands warp in a manner where there is no significant contribution towards the double resonance process. This discussion assumes a uniform coverage and a well-ordered film. However, as discussed below, the surface and buffer layer have complicated geometric structures with a relatively high density of SiC steps and domains of different graphene thickness. These features and domains may also influence the intensity of the 2D-band, especially after exposure to atmosphere.

Room temperature STM images of low-coverage EG grown on Si-terminated SiC (0 0 0 1) are shown in Fig. 5a–c. These correspond to layer 0, layer 1, and layer 2 respectively on nominal 2.3 ML_e EG on SiC (0 0 0 1). The tunnel voltage in these images was chosen to enable imaging of both the graphene lattice and the subsurface interface states [39]. In the empty state image of layer 0 (Fig. 5a), we do not observe any evidence of the graphene lattice. Bias dependent imaging of this buffer layer also did not reveal any structural similarities with graphene, consistent with the reduced π-band density-of-states found in ARPES [9]. Fig. 5b is a filled-states image (−0.5 V sample bias) of layer 1 that shows the unique character of the STM "topography", which is dominated by position-dependent variations in the local density-of-states due to the subsurface (layer 0) reconstruction. At higher tunnel bias, the image can be completely dominated by the interface states [39,40]. Throughout the image, a network of sp^2-bonded C atoms is evident as an underlying honeycomb pattern. We observe a step-height of ~2.4 Å from layer 0 to layer 1, consistent with calculations and recent surface X-ray reflectivity measurements [15], but much smaller than the 3.41 Å interlayer spacing in graphite. This suggests substantial interaction between the interface layer 0 and the layer 1 graphene. In the layer 2 filled-states image shown in Fig. 5c, the graphene atomic lattice is also observed, but the two sublattice atoms in the honeycomb do not image identically. This bias-dependent phenomenon is an indication of Bernal stacking of the two layers [41], which breaks the sublattice degeneracy. Also evident in Fig. 5c is a superimposed modulation of the graphene surface height. This 6×6 period is due to the deformation of the graphene sheet as it blankets layer 1 and the interface reconstruction [42]. We point out that epitaxial graphene layers are always observed to be continuous over step edges, whether over substrate steps, or steps between different EG layers (excepting layer 0 to layer 1 transitions, since graphene was not imaged in layer 0). This is also the case for small raised domains of layer 2 material occasionally observed within an otherwise layer 1 terrace (for such islands the step-height between layers 1 and 2 is 3.4 Å, essentially the same as the interlayer spacing of graphite). These observations suggest that substantial lateral diffusion occurs, perhaps both on top of the graphene layer and underneath.

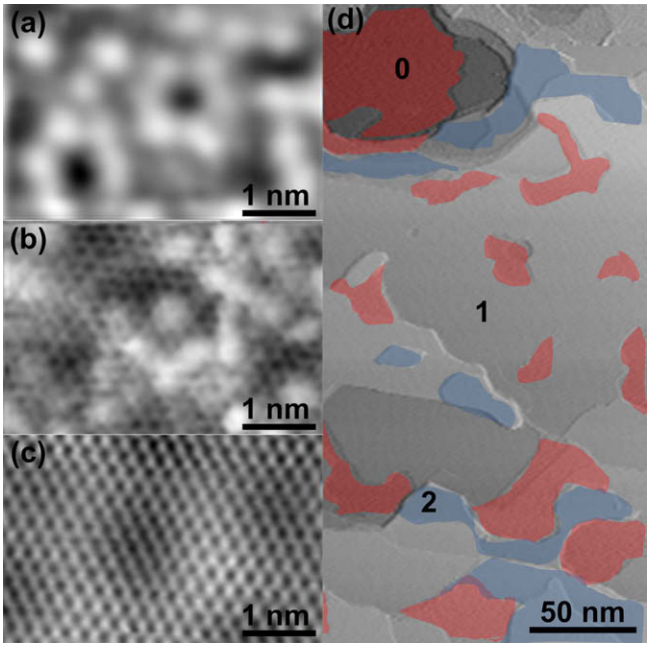

Fig. 5. STM images of the EG sample on the SiC substrate grown by thermal annealing under UHV conditions. The images are acquired at a constant tunneling current of 100 pA. (a) and (b) are 46 × 43 Å STM images of layer 0 and layer 1 EG at biases of 0.4 V and 0.5 V, respectively. Figure (a) shows features that do not match the graphene lattice; (b) shows the graphene lattice, along with adatom like interface features due to interface states from layer 0; and (c) shows layer 2 graphene having a 6×6 period superimposed. The 6×6 atomic corrugation is due to graphene draping over the interface features. (d) 1500 Å × 2700 Å STM survey image of a 2.3 ML_e sample. The layer 0 and 2 regions are marked with red and blue overlays, respectively, while layer 1 is unshaded (gray height scale). Although the sample is dominated by layer 1 in this particular region, the average effect is measured in Raman spectra. (For interpretation of the references to colour in this figure legend, the reader is referred to the web version of this article.)

STM survey scans on the samples prepared for Raman measurements indicate differences in the thickness and domain size of graphene. Even though the topmost graphene layer always appears continuous in STM, substrate steps apparently seed many transitions in graphene layer thickness. A correlation was observed between the domain size and the intensity of the D peak for two samples prepared under nominally identical conditions (the sample having smaller domains had a larger D peak). Note that

the initial SiC surface (after hydrogen etching) consists of a regular array of 1.5-nm-high steps (one unit cell) separated by ~600 nm terraces, consistent with the vicinality of the substrate [8]. Most of the steps observed in Fig. 5d are steps in the SiC substrate that form during graphitization [14]. The surface coverage (determined from many additional images) is approximately 50% layer 2 material. Counting only layers 1 and 2 (those that image as a carbon honeycomb) the actual graphene coverage of this sample is ~1.5 ML. The difference of 0.8–1.0 ML between the AES film thickness and the graphene coverage determined by STM implies that layer 0 is carbon rich. Although the detailed structure of this interface layer is not known [9,21,43], the surface X-ray reflectivity is best fit by a model where the transition spans one SiC bilayer (in which carbon largely replaces Si) plus a low-density predominantly Si adatom layer [15,39].

4. Conclusions

Epitaxial graphene layers thermally grown on Si-terminated 6H-SiC (0 0 0 1) have been probed using Auger electron spectroscopy, Raman microspectroscopy and scanning tunneling microscopy. Systematic changes in the Raman spectra are observed as the film thickness increases from 1 to 3 layers. Correlating the Raman spectral information with STM images, we show that the first graphene layer imaged by STM produces no 2D peak, but the second imaged layer shows a single-Lorentzian 2D peak near 2750 cm^{-1}, similar to spectra acquired from single-layer micromechanically cleaved graphene on SiO_2. The 4–10 cm^{-1} higher frequency shift of the G peak relative to CG can be associated with charge exchange with the underlying SiC substrate and the formation of finite size domains of graphene. The much greater (41–50 cm^{-1}) blue shift observed for the 2D-band for thicknesses >1.8 ML_e may be correlated with these domains and with compressive strain. In general, the >1.8 ML_e epitaxial graphene layers are observed to be continuous over step edges, whether over substrate steps, or steps between different EG layers. This is also the case for small raised domains of layer 2 material.

Acknowledgments

The authors wish to acknowledge M. Sprinkle for help in preparing SiC substrates and W.A. de Heer for useful conversations. This work was supported by National Science Foundation Grants ECCS-0404084 (NIRT) and DMR-0804908. Use of facilities within the Georgia Tech Laboratory for New Electronic Materials (NSF MRSEC DMR-0820382) is also acknowledged.

References

[1] K.S. Novoselov et al., Science 306 (2004) 666.
[2] Y. Zhang et al., Phys. Rev. Lett. 96 (2006) 142806.
[3] K.S. Novoselov et al., Nat. Phys. 2 (2006) 177.
[4] M.I. Katsnelson, K.S. Novoselov, A.K. Geim, Nat. Phys. 2 (2006) 620.
[5] E. McCann, Phys. Rev. B 74 (2006) 161436.
[6] C. Berger et al., J. Phys. Chem. B 108 (2004) 19912.
[7] C. Berger et al., Science 312 (2006) 1191.
[8] W.A. de Heer et al., Solid State Commun. 143 (2007) 92.
[9] K.V. Emtsev, F. Speck, T. Seyller, L. Ley, J.D. Riley, Phys. Rev. B 77 (2008) 155303.
[10] G.M. Rutter et al., Science 317 (2007) 219.
[11] A. Bostwick, T. Ohta, T. Seyller, K. Horn, E. Rotenberg, Nat. Phys. 3 (2007) 42.
[12] T. Ohta, A. Bostwick, T. Seyller, K. Horn, E. Rotenberg, Science 313 (2006) 951.
[13] S.Y. Zhou et al., Nat. Mat. 6 (2007) 770.
[14] J. Hass et al., Appl. Phys. Lett. 89 (2006) 143106.
[15] J. Hass, J.E. Millan-Otoya, P.N. First, E.H. Conrad, Phys. Rev. B 78 (2008) 205424.
[16] Z.H. Ni et al., Phys. Rev. B 77 (2008) 115416.
[17] D.S. Lee et al., Nano Lett. 8 (2008) 4410.
[18] C. Faugeras et al., Appl. Phys. Lett. 92 (2008) 011914.
[19] N. Ferralis, R. Maboudian, C. Carraro, Phys. Rev. Lett. 101 (2008) 156801.
[20] J. Rohrl et al., Appl. Phys. Lett. 92 (2008) 201918.
[21] Th. Seyller et al., Surf. Sci. 600 (2006) 4206.
[22] L.I. Johansson, F. Owman, P. Martensson, Phys. Rev. B 53 (1996) 14423.
[23] J. Algdal, T. Balasubramanian, M. Breitholtz, T. Kihlgren, L. Wallden, Surf. Sci. 601 (2007) 1167.
[24] C. Thomsen, S. Reich, Phys. Rev. Lett. 85 (2000) 5214.
[25] A.C. Ferrari et al., Phys. Rev. Lett. 97 (2006) 187431.
[26] CREE, CREE Inc., 2004.
[27] SPI, SPI Supplies Grade SPI-1, 2007.
[28] T. Li, Ph.D. Thesis, Georgia Institute of Technology, 2006. <http://etd.gatech.edu/theses/available/etd-11172006-170042/>.
[29] G. Ertl, J. Kuppers, Low Energy Electrons and Surface Chemistry, VCH Publishers, 1985.
[30] S. Tanuma, C. Powell, D. Penn, Surf. Interf. Anal. 17 (1991) 911.
[31] A.C. Ferrari, Solid State Commun. 143 (2007) 47.
[32] L.G. Cancado et al., Appl. Phys. Lett. 88 (2006) 163106.
[33] L.G. Cancado et al., Phys. Rev. Lett. 93 (2004) 24701.
[34] S. Pisana et al., Nat. Mat. 6 (2007) 198.
[35] A. Das et al., Nat. Nanotechnol. 3 (2008) 210.
[36] J. Kurti, V. Zolyomi, A. Gruneis, H. Kuzmany, Phys. Rev. B 65 (2002) 165442.
[37] S. Piscanec, M. Lazzeri, F. Mauri, A.C. Ferrari, J. Robertson, Phys. Rev. Lett. 93 (2004) 185503.
[38] J. Maultzsch, S. Reich, C. Thomsen, Phys. Rev. B 70 (2004) 155436.
[39] G.M. Rutter et al., Phys. Rev. B 76 (2007) 241416.
[40] C. Riedl, U. Starke, J. Bernhardt, M. Franke, K. Heinz, Phys. Rev. B 76 (2007) 245439.
[41] G.M. Rutter, J.N. Crain, N.P. Guisinger, P.N. First, J.A. Stroscio, J. Vac. Sci. Technol. A 26 (2008) 941.
[42] P. Lauffer et al., Phys. Rev. B 77 (2008) 155426.
[43] J.B. Hannon, R.M. Tromp, Phys. Rev. B 77 (2008) 4.